Available online at www.sciencedirect.com

ScienceDirect

IFAC PapersOnLine 59-30 (2025) 191–196

On Wind Estimation Techniques for Airborne Wind Energy Systems

Matteo Bordignon * **Alessandro Croce** ** **Lorenzo Mario Fagiano** ***

* *Department of Aerospace Science and Technology, Politecnico di Milano, Milan, Italy (e-mail: matteo.bordignon@polimi.it)*
** *Department of Aerospace Science and Technology, Politecnico di Milano, Milan, Italy (e-mail: alessandro.croce@polimi.it)*
*** *Department of Electronics, Information and Bioengineering, Politecnico di Milano, Milan, Italy (e-mail: lorenzo.fagiano@polimi.it)*

Abstract: Airborne Wind Energy (AWE) exploits kites for high-altitude power generation but faces control challenges due to system complexity and wind uncertainty. Accurate wind estimation at operational altitude is essential, yet current methods like extrapolation and EKF present significant drawbacks. This work proposes two novel, generalizable estimation techniques requiring only minimal sensor data (kite position, tether force). One employs optimization on a simplified model, while the second solves a linear system derived from specific dynamic assumptions, suitable for least-squares or Kalman filtering. Both methods are tested using real flight data and compared with surface wind speed measurements.

Keywords: Estimation and filtering, Airborne Wind Energy, Gradient-based Optimization, Wind speed, Least-squares, Kalman Filter

1. INTRODUCTION

Airborne Wind Energy (AWE) is a technology able to harness wind power by employing an autonomous tethered aircraft, usually referred to as a kite. Systems within this category can harvest higher-altitude wind energy (approximately 200-500 m from the ground), resulting in a high power yield and reduced material usage, as first theoretically introduced by Loyd (1980). However, this advantage comes at the cost of a higher system complexity compared to the more traditional wind turbines. The role of automation is, therefore, crucial in order to exploit the benefits of this technology. System reliability poses a primary challenge, as highlighted by Fagiano et al. (2021), mainly due to the complexities of its coupled dynamics and the inherent uncertainty of environmental conditions. These factors complicate the development of efficient and robust control strategies. Consequently, the incorporation of accurate, real-time wind speed measurement at the operational altitude could offer substantial benefits both in the control systems' effectiveness and fault tolerance, given that wind is the primary source of power while simultaneously being the main source of disturbance in the system.

This problem calls for the need of estimation and filtering procedures, since the rapid dynamics of kites render traditional wind speed sensors, such as pitot tubes, ineffective. Currently employed methodologies follow two main paths. The most straightforward one is based on a simple extrapolation of operation altitude winds based on ground-level measurements. The relationship between the two is, however, complex, non-linear, and highly variable, strongly influenced by several factors, such as atmospheric stability, surface roughness, and terrain complexity. Therefore, this approach, depicted by empirical models like the logarithmic and power laws, often produces inaccurate and unreliable results. The second methodology employed an Extended Kalman Filter (EKF) or its different variations. In particular, Ranneberg (2013) proposes the use of an Unscented Kalman Filter to estimate both the kite states and the wind characteristics. A comprehensive summary of the existing approaches is provided in Cayon et al. (2025), which also introduces a novel application of this approach. Despite the advantages of the EKF-based approach, it presents several challenges in its practical implementation. First, filter tuning is required, making the system susceptible to the choice of numerous estimation parameters, which can be challenging to determine optimally. Second, the approach often employs an ad-hoc model, meaning that the system dynamics must be carefully defined for each specific setup, reducing its generalizability. Finally, the computational burden of this method is significant, limiting its feasibility for lightweight and embedded control systems. These drawbacks highlight the need for alternative wind estimation techniques that can achieve both accuracy and efficiency while minimizing complexity.

This paper proposes and compares two alternative design philosophies in wind estimation methods developed with simplicity, generalizability, and minimal sensor requirements as primary goals, addressing the limitations underlined in the aforementioned techniques. Indeed, both approaches rely solely on easily retrievable data, such as kite position, along with its derivatives, and tether force. All of the measurements are easily retrievable in a real-world setting, therefore making the method practically feasible. Exploiting a simplified model of the system, the

10.1016/j.ifacol.2025.12.235

first method formulates an optimization problem to find the wind conditions that minimize the error between predicted and measured system behavior. The second one employs specific assumptions about the system's attitude and dynamics to obtain a system of equations that is linear with respect to the wind magnitude, allowing a direct solution via least-squares or suitable for implementation in a Kalman Filter (KF) framework.

Notation and units Vectors will be denoted by **bold** characters, while their Euclidean norm will be indicated with $\|.\|$. Parameters specific to the kite and the tether will be denoted, respectively, with the superscripts k and t. The components (x, y, z) of a generic vector $\boldsymbol{r}$ will be represented as r_x, r_y and r_z respectively. Additionally, if the value of a generic variable v is measured, it will be depicted by $\tilde{v}$.

2. OPTIMIZATION-BASED WIND ESTIMATION

This first method addresses the wind estimation problem using a Gradient-Based Optimization technique, which is part of a broader class of methods that leverage first and second-order optimality conditions to identify the minimum of a given cost function. In particular, this work employed a *Sequential Quadratic Programming* (SQP) method that uses *Broyden–Fletcher–Goldfarb–Shanno* (BFGS), a quasi-Newton method, to approximate the Hessian matrix. This approximation is essential for verifying whether the best candidate solution satisfies the second-order optimality condition. Through the use of BFGS, the Hessian matrix can be estimated efficiently using only gradient information from the cost function and constraints.

2.1 Estimation model

Central to this technique is an estimation model, chosen through a trade-off between fidelity and generalizability. The objective was to capture the core dynamics of a rigid or flexible wing connected to the ground via one or multiple tethers, relevant to most AWE systems, avoiding over-specialization to a single configuration, therefore improving the versatility of the method. This model serves as a computationally efficient representation of a more complex, higher-fidelity model rigorously detailed by Fagiano (2009). Figure 1 provides a schematic representation of the system configuration considered.

A single equivalent point mass, denoted with m, was employed to represent the combined effects of various forces acting on the system. This point is positioned at the kite's aerodynamic center, denoted with vector $\boldsymbol{r}$, and lumps both the kite's mass m^k and an effective mass representing the tether m^t. The total mass used for inertial calculation is

$$m = m^k + \frac{1}{2}m^t = m^k + \frac{1}{2}n^t 2\pi(d^t)^2\mu^t \qquad (1)$$

where n^t, d^t, μ^t are the characteristics of the tether system, respectively number of tethers, tether diameter, and tether density. Note that the position of the point mass could also be defined in spherical coordinates using the azimuth angle ϕ, the elevation angle θ, and the tether length L. Moreover, the model assumes a taut tether during the operation. Therefore, the length of the tether can be expressed as $L = \|\boldsymbol{r}\|$.

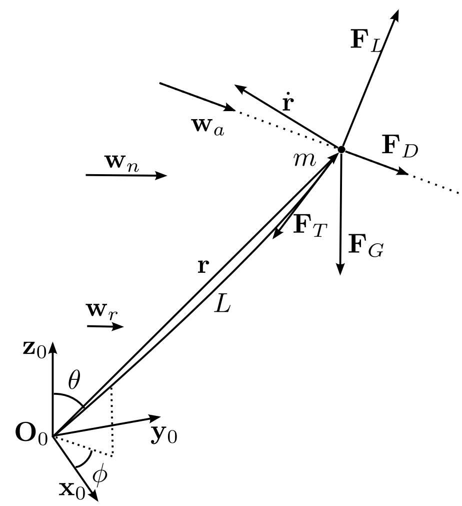

Fig. 1. Diagram of the point mass AWE system model, illustrating the kite position vector $\boldsymbol{r}$, the ground-fixed reference frame (X,Y,Z) with unit vectors $(\boldsymbol{x}_0, \boldsymbol{y}_0, \boldsymbol{z}_0)$, and relevant forces acting on the point mass m

The system will be described within an inertial reference frame fixed to the ground station where the tether is attached. This reference frame, denoted as $R = (X, Y, Z)$, is right-handed, with X representing the primary wind direction, Z pointing upward, and Y completing the coordinate system. In Figure 1, this reference frame is illustrated using its unit vectors $\boldsymbol{x}_0$, $\boldsymbol{y}_0$, and $\boldsymbol{z}_0$.

The primary forces acting on the point mass m are modeled as follows: aerodynamic lift $(\boldsymbol{F}_L)$, aerodynamic drag $(\boldsymbol{F}_D)$, gravity $(\boldsymbol{F}_G)$, and tether tension $(\boldsymbol{F}_T)$.

The aerodynamic forces depend on the apparent wind velocity $\boldsymbol{w}_a$, defined as the velocity of the wind relative to the kite:

$$\boldsymbol{w}_a = \boldsymbol{W} - \dot{\boldsymbol{r}} \qquad (2)$$

where $\boldsymbol{W}$ is the absolute wind velocity vector acting on the point mass and $\dot{\boldsymbol{r}}$ is the kite's velocity vector.

The aerodynamic and gravitational forces are given by:

$$\boldsymbol{F}_L = \frac{1}{2}\rho A\overline{C_L}\|\boldsymbol{w}_a\|^2\boldsymbol{z}_l \qquad (3)$$

$$\boldsymbol{F}_D = \frac{1}{2}\rho A\overline{C_D}\|\boldsymbol{w}_a\|^2\frac{\boldsymbol{w}_a}{\|\boldsymbol{w}_a\|} \qquad (4)$$

$$\boldsymbol{F}_G = (m^k + \frac{1}{2}m^t)\begin{bmatrix}0\\0\\-g\end{bmatrix} = mg\boldsymbol{z}_0 \qquad (5)$$

$$(6)$$

Here, ρ is the air density, A is the characteristic wing area, C_L and C_D are the mean lift and drag coefficients, g is the acceleration due to gravity, and $\boldsymbol{z}_l$ is the unit vector defining the lift force direction. The explicit definition of $\boldsymbol{z}_l$ is necessary as the lift force acts perpendicularly to the relative airflow direction, hence, it's not uniquely defined by it but lies in its orthogonal plane.

The tether force $\boldsymbol{F}_T$ acts along the tether line towards the ground station. Under the previously introduced assumption of taut and inelastic tether:

$$\boldsymbol{F}_T = \|\tilde{\boldsymbol{F}_T}\| \frac{\tilde{\boldsymbol{r}}}{L} \tag{7}$$

where $\|\tilde{\boldsymbol{F}_T}\|$ is the magnitude of the tension force, considered as a given measurement of the system.

Applying Newton's second law to the point mass m yields the equation of motion:

$$\ddot{\boldsymbol{r}} = \frac{\boldsymbol{F}_L + \boldsymbol{F}_D + \boldsymbol{F}_G - \boldsymbol{F}_T}{m} \tag{8}$$

where $\ddot{\boldsymbol{r}}$ is the acceleration vector of the point mass. The negative sign for $\boldsymbol{F}_T$ represents the force *on* the mass by the tether, which acts radially inwards.

The overall system dynamics can be summarized in the form:

$$\ddot{\boldsymbol{r}} = f_{est}(\tilde{\boldsymbol{r}}, \dot{\tilde{\boldsymbol{r}}}, \|\tilde{\boldsymbol{F}_T}\|, \overline{\boldsymbol{p}}, \boldsymbol{W}, \boldsymbol{z_l}) \tag{9}$$

where $\overline{\boldsymbol{p}} = [\rho, A, \overline{C_L}, \overline{C_D}, m^k, n^t, d^t, \mu^t]$ is the vector of constant parameters representing the system's physical properties.

2.2 Optimization problem

By defining the direction of the lift vector $\boldsymbol{z_l}$ and the absolute wind vector $\boldsymbol{W}$ through their respective directional components

$$\boldsymbol{z_l} = [z_{lx}\ z_{ly}\ z_{lz}]^T \tag{10}$$

$$\boldsymbol{W} = [W_x\ W_y\ W_z]^T \tag{11}$$

and by assuming no wind along the vertical direction, it's possible to define the vector of optimization variables as

$$\boldsymbol{u} = [W_x\ W_y\ z_{lx}\ z_{ly}\ z_{lz}]^T \tag{12}$$

At each time step, the following nonlinear optimization problem is solved. It tries to minimize the difference between the measured accelerations of the kite and the computed ones from the estimation model. An additional term is added to the cost function based on the difference between the solution at the current step and the previous step.

$$\begin{aligned}
\underset{\boldsymbol{u}}{\text{minimize}} \quad & (\ddot{\tilde{\boldsymbol{r}}} - \ddot{\boldsymbol{r}})^T Q (\ddot{\tilde{\boldsymbol{r}}} - \ddot{\boldsymbol{r}}) + && \text{(13a)}\\
& (\boldsymbol{u} - \boldsymbol{u}_{old})^T Q_{diff} (\boldsymbol{u} - \boldsymbol{u}_{old}) && \text{(13b)}\\
\text{subject to} \quad & \ddot{\boldsymbol{r}} = f_{est}(\tilde{\boldsymbol{r}}, \dot{\tilde{\boldsymbol{r}}}, \|\tilde{\boldsymbol{F}_T}\|, \boldsymbol{p}, \boldsymbol{u}), && \text{(13c)}\\
& \underline{\boldsymbol{u}} \leq \boldsymbol{u} \leq \overline{\boldsymbol{u}}, && \text{(13d)}\\
& \|\boldsymbol{z_l}\| - 1 = 0, && \text{(13e)}\\
& \boldsymbol{z_l}^T \boldsymbol{w_a} = 0 && \text{(13f)}
\end{aligned}$$

The optimization problem defined in (13) incorporates several constraints to ensure physical realism and adherence to aerodynamic principles:

- *Box Constraints* (13d)*:* These inequality constraints define the feasible range for each component of the optimization vector $\boldsymbol{u}$. The lower bounds $\underline{\boldsymbol{u}}$ and upper bounds $\overline{\boldsymbol{u}}$ restrict the estimated wind components (W_x, W_y) and lift direction components (z_{lx}, z_{ly}, z_{lz}) to physically meaningful or expected intervals. For instance, wind speed limits might be imposed, and the components of $\boldsymbol{z_l}$ are inherently bounded between -1 and 1, although these bounds could be tighter based on operational expectations.
- *Unit Vector Constraint* (13e)*:* This equality constraint, enforces the mathematical definition of $\boldsymbol{z_l}$ as a unit vector. Since z_{lx}, z_{ly}, z_{lz} are components of $\boldsymbol{u}$, this ensures that the optimization yields a valid direction vector for the lift force.
- *Lift Orthogonality Constraint* (13f)*:* This final equality constraint represents the fundamental aerodynamic principle behind the introduction of $\boldsymbol{z}_l$: the lift force vector must be orthogonal to the apparent wind velocity vector $\boldsymbol{w_a}$. Since the apparent wind $\boldsymbol{w_a}$ depends on both the estimated absolute wind $\boldsymbol{W}$ and the measured kite velocity $\dot{\tilde{\boldsymbol{r}}}$, this constraint creates an important coupling between the variables being optimized and the known state of the system.

These constraints collectively define the feasible search space for the optimization variables, ensuring that the solution not only minimizes the cost function but also respects the underlying physics and definitions of the system model.

3. WIND ESTIMATION BASED ON LINEAR REGRESSION AND FILTERING

In this section, alternative wind estimation techniques are presented, based on Least-Squares principles and Kalman filtering. As presented in Fagiano et al. (2012) and summarized here, by adopting suitable simplifying assumptions, it is possible to derive a reduced set of kite equations. These assumptions rely on the fact that the kite is flying in a crosswind configuration and that the lift force is responsible for maintaining tension in the tether.
From the simplified equations, a direct relationship can be established between the magnitude of the apparent wind vector projected onto the tether, $|\boldsymbol{W_{e,t}}|$, and the traction force, $\|\tilde{\boldsymbol{F}_T}\|$, which can be readily measured by onboard sensors. This yields the relationship:

$$|\boldsymbol{W_{e,t}}| = \sqrt{\frac{\|\tilde{\boldsymbol{F}_T}\|}{\frac{1}{2}\rho A C_L E_{eq}^2 \left(1 + \frac{1}{E_{eq}^2}\right)^{3/2}}} = \sqrt{\frac{\|\tilde{\boldsymbol{F}_T}\|}{C}} \tag{14}$$

where

$$E_{eq} = \frac{\|\boldsymbol{F}_L\|}{\|\boldsymbol{F}_{D,tot}\|} = \frac{C_L}{C_{D.eq}} \tag{15}$$

$$C_{D.eq} = C_D \left(1 + \frac{n^t\, L\, d^t\, C_D^t}{4\, A\, C_D}\right) \tag{16}$$

Once $|\boldsymbol{W_{e,t}}|$ has been computed, it can be used to create a relationship between the magnitude of the absolute wind vector components, resulting in the following equation, linear in these components:

$$W_x l_x(t) + W_y l_y(t) + W_z l_z(t) - \dot{L} = |\boldsymbol{W_{e,t}}| \tag{17}$$

where $\boldsymbol{l}$ is the unit vector of the kite position, expressed as

$$\boldsymbol{l} = \frac{\boldsymbol{r}}{L} = [l_x\ l_y\ l_z]^T \tag{18}$$

and $\dot{L}$ is the reel-out speed of the tether.

The linear relationship expressed in 17 forms the basis for the wind estimation techniques explored in this work: a direct least-squares approach and a Linear Kalman filter implementation.

3.1 Least-squares implementation

By assuming that the wind remains constant over a time window, a system of linear equations based on 17 can be defined. Specifically solving for W_x and W_y, a direct solution of the system can be found if, under the assumption of the absence of wind in the vertical direction ($W_z = 0$), the time window is set to $N = 2$. A further increase in the window size ($N > 2$) produces an overdetermined system that can be solved using a sliding-window least-squares approach to reconstruct the wind vector at each time step. The system takes the form

$$\mathbf{A}_k \mathbf{W}_k \approx \mathbf{b}_k \tag{19}$$

where $A_k \in \mathbb{R}^{N\times 2}$ contains rows $[l_x(\tau), l_y(\tau)]$ and $b_k \in \mathbb{R}^N$ contains elements $|\boldsymbol{W}_{\boldsymbol{e},\boldsymbol{t}}|$, for $\tau = k - N + 1, \ldots, k$. The least-squares solution minimizes $\|\mathbf{A}_k \mathbf{W}_k - \mathbf{b}_k\|^2$.
A critical limitation is that the constant wind assumption is invalid during the kite's turning maneuvers. Therefore, the estimation method must be restricted to the quasi-straight segments of the figure-eight trajectory. Identifying these periods requires an indicator that balances accessibility with reliable turn detection. This study found the magnitude of the azimuth angle's derivative, $\|\dot{\phi}\|$, to be an effective indicator, as low values directly correspond to slow horizontal movements characteristic of turns. Data samples are therefore filtered using a threshold on $\|\dot{\phi}\|$; only estimation windows where all N samples satisfy the straight-flight condition (e.g., $\|\dot{\phi}(\tau)\| \le \phi_{threshold}$ for $\tau = k-N+1, \ldots, k$) values are utilized for wind reconstruction. Despite these limitations, this method has demonstrated comparable estimation results and significant computational advantages over the previous approach, achieving a 20- to 30-fold improvement in computation time.

3.2 Kalman Filter implementation

Alternatively, the wind estimation problem can be formulated within a state-space framework using a linear Kalman filter. This approach leverages Equation 17 (under the $W_z = 0$ assumption) for the measurement update and allows for the incorporation of a dynamic model for wind evolution and explicit handling of process and measurement noise.
A discrete-time Kalman filter is used to estimate the two-dimensional wind vector components, denoted as the state vector $\mathbf{x}_k = [W_x(k), W_y(k)]^T$, at time step k. Within the filter, it is assumed a random walk process model for the wind dynamics, implying the state transition matrix is the identity matrix ($\mathbf{F} = \mathbf{I}$). The prediction step thus simplifies to

$$\hat{\mathbf{x}}_{k|k-1} = \hat{\mathbf{x}}_{k-1|k-1} \tag{20}$$

The uncertainty in this prediction is modeled by the process noise covariance matrix $\mathbf{Q}$, defined as a diagonal matrix $\mathbf{Q} = \mathrm{diag}(\sigma^2_{w_x}\Delta t, \sigma^2_{w_y}\Delta t)$, accounting for independent

Fig. 2. Experimental setup of UC Santa Barbara $12m^2$ Prototype. (1) Kite, (2) Tethers, (3) Sensor estimating elevation θ and azimuth ϕ, (4) One of the three tether force sensors

stochastic variations in each wind component scaled by the estimation time step Δt.
The filter leverages the scalar measurement $z_k = |\boldsymbol{W}_{e,r}(k)|$, which is related to the state via the previously obtained linear equation 17. This forms the basis of the measurement model

$$z_k = \mathbf{H}_k^T \mathbf{x}_k - \dot{L}_k + v_k \tag{21}$$

where $\mathbf{H}_k = [l_x(k), l_y(k)]^T$ is the time-varying measurement matrix derived from the position unit vector components and v_k is the measurement noise, assumed to be zero-mean Gaussian with variance R_k.
A key feature is the adaptive measurement noise variance $R_k = \mathbb{E}[v_k^2]$. This variance is adjusted based on turn detection, similar to the previous approach, assigning a higher variance during turns compared to straight segments to reflect potentially degraded measurement quality. This effectively de-weights measurements during maneuvers where the underlying linear model assumptions may be violated.

4. EXPERIMENTAL RESULTS

The performance of the three wind estimation methods – Least Squares (LS), Optimization (OPT), and Kalman Filter (KF) – was evaluated using both simulated data and real flight data. The real data originates from field tests of the 12m^2 kite prototype developed at the University of California, Santa Barbara. Figure 2 depicts the experimental setup. Simulated data was generated using the comprehensive Airborne Wind Energy (AWE) system model detailed in Fagiano (2009). To specifically highlight the methods' response characteristics, the simulated wind speed history included a manually inputted double step change. In the simulation environment, the true wind speed was known and used as a reference. For the real flight tests, only ground-based wind measurements were available. However, as the kite operated at an approximate altitude of 30 meters, the wind speed at this height is assumed to be reasonably similar to the ground measurements. Notably, this same flight dataset was also analyzed in Schmidt et al. (2020), where an Extended Kalman Filter (EKF) was used for comparison. Figures 3 and 4 illustrate the results achieved by the three methods, displaying how the methods estimate the wind speed magnitude, taken as the norm of the estimated wind vector.

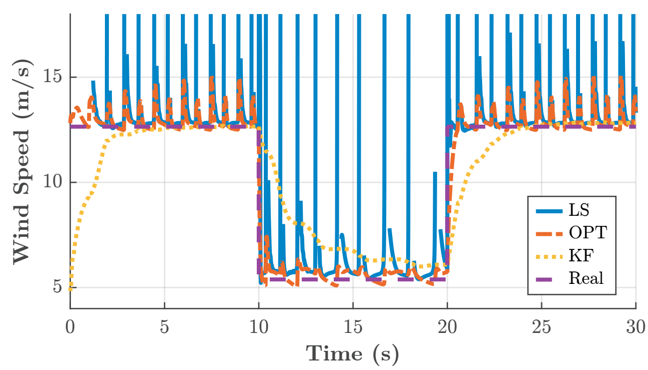

Fig. 3. Wind magnitude estimation results in simulation. The three methods (LS, OPT, and KF) are compared with the reference magnitude at the trajectory height.

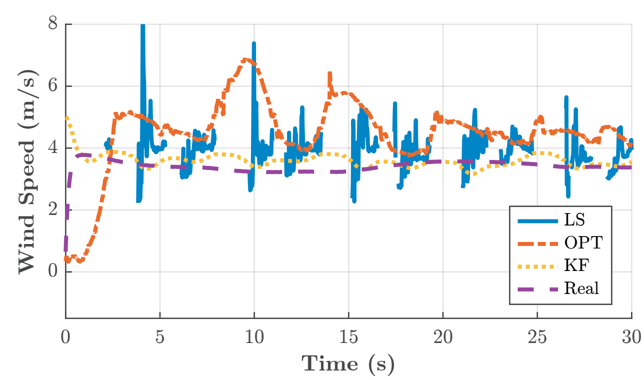

Fig. 4. Wind magnitude Estimation results with the $12m^2$ kite of the UCSB prototype during a field experiment.

Observing the simulation results (Fig. 3), the LS method exhibits significant spikes. As previously presented, these occur primarily when the kite approaches the turning phases of its trajectory. In these regions, several modeling assumptions are violated. Specifically, the linear model assumptions outlined in Section 3 become less valid. Furthermore, the assumption of constant average lift ($\overline{C}_L$) and drag ($\overline{C}_D$) coefficients deviates from reality, as the angle of attack changes rapidly during turns. Unmodeled centrifugal effects, which become increasingly significant during turns, also contribute to these estimation errors.
In contrast, the KF implementation, benefiting from its adaptive measurement noise variance, shows greater robustness during turning phases and avoids the large spikes seen with the LS method. However, this robustness comes at the cost of slower convergence to the true wind speed magnitude following the step changes.
The optimization-based (OPT) method yielded performance that shared characteristics with both LS and KF. It displayed transient spiking behavior similar to the LS method, although generally less pronounced. It is important to underline that this occurred even though the OPT estimation model did not incorporate explicit information regarding turning maneuvers or rely on flight behavior assumptions. Nevertheless, the reliance on constant values of the aerodynamic coefficients persisted, likely contributing to the oscillatory behavior observed, particularly visible in the real data results shown in Figure 4.
Beyond estimation accuracy, the methods differ considerably in terms of computational demand and tuning effort. As expected, the OPT approach proved the most computationally intensive, necessitating the solution of a constrained optimization problem involving five variables and several constraints at each time step. Consequently, its execution time was approximately an order of magnitude greater than that of the LS and KF methods, which exhibited comparable computational efficiency.
Regarding ease of implementation, the LS method required the least tuning, primarily involving the selection of the sliding window size (N). This parameter selection concerns the balancing of estimation smoothness (favored by larger N) against the validity of the constant wind assumption over the window's duration. The KF required careful tuning of its noise covariance matrices, especially the adaptive measurement noise variance R_k, which critically influences filter behavior during straight flight and turning maneuvers. The OPT method presented the most significant tuning challenge; its performance proved highly sensitive to the precise values chosen for the weighting matrices Q and Q_{diff} within the optimization cost function, requiring considerable effort to achieve optimal results.

To provide quantitative metrics supporting these observations, Table 1 summarizes the Root Mean Square Error (RMSE) of the wind magnitude estimation and the computational time required for each method when processing a 60-second segment of the real flight data.

Table 1. Estimation RMSE and computational burden on a 60-second real flight data sample

	RMSE	**Comp. Time**
OPT	1.587	68.890 s
LS	2.213	1.736 s
KF	0.584	0.038 s

The results in Table 1 quantify the trade-offs discussed: the KF achieves the lowest RMSE and computational time for this dataset, while the OPT method shows a significantly higher computational cost, requiring more time than the duration of the data segment itself. The LS method presents a middle ground in terms of computational time but exhibits the highest RMSE among the three in this specific real-data scenario, consistent with the oscillations observed in Figure 4.

5. CONCLUSIONS

This research addresses the critical need for accurate, real-time wind estimation in Airborne Wind Energy systems, highlighting the practical challenges and limitations of existing methods like simple extrapolation and computationally intensive Extended Kalman Filters. Two lightweight alternative wind estimation techniques were proposed, prioritizing generalizability and minimal sensor requirements (relying only on kite position and tether force measurements).

The first method employed a gradient-based optimization (OPT) approach on a simplified point-mass model to minimize the discrepancy between modeled and measured kite dynamics. The second method derived a linear relationship between wind components and measured tether force under specific dynamic assumptions, enabling solutions via both a sliding-window Least Squares (LS) approach and a linear Kalman Filter (KF) with adaptive noise variance.

Experimental validation using both simulated and real flight data demonstrated various performance characteristics for each method:

- The LS method proved computationally efficient and simple to tune, but exhibited significant estimation errors in the form of spikes during kite turning maneuvers where its underlying assumptions were violated despite an a priori threshold filtering.
- The KF method offered improved robustness during turns by adaptively adjusting measurement noise, mitigating the large spikes seen in LS, though it showed slower convergence to abrupt wind changes and required more careful tuning.
- The OPT method showed performance intermediate between LS and KF, with less pronounced spiking than LS during turns, but was the most computationally demanding and sensitive to tuning parameters.

Future works starting from this paper could include a direct and quantitative comparison with EKF-based methods to rigorously benchmark the trade-offs between the proposed simplified estimators and state-of-the-art approaches, the exploration of hybrid models that could switch between estimation strategies depending on the flight regime and the use of such methods to estimate the wind field of the area swept by the system.

The study successfully developed and compared novel wind estimation techniques requiring only basic and readily available AWE system measurements. The findings underscore a trade-off between estimation accuracy, robustness, computational cost, and tuning effort, offering guidance for selecting suitable, minimally sensor-dependent wind estimation strategies for AWE control.

ACKNOWLEDGEMENTS

This research has been partially supported by the MERIDIONAL project, which receives funding from the European Union's Horizon 2020 program (grant agreement no. 101084216).

REFERENCES

Cayon, O., Watson, S., and Schmehl, R. (2025). Kite as a Sensor: Wind and State Estimation in Tethered Flying Systems. *Wind Energy Science Discussions*, 1–41. doi: 10.5194/wes-2024-182. Publisher: Copernicus GmbH.

Fagiano, L. (2009). *Control of tethered airfoils for high-altitude wind energy generation.* Ph.d. dissertation, Politecnico di Torino, Turin, Italy. Available: http://hdl.handle.net/11311/1006424.

Fagiano, L., Milanese, M., and Piga, D. (2012). Optimization of airborne wind energy generators. *International Journal of Robust and Nonlinear Control*, 22(18), 2055–2083. doi:10.1002/rnc.1808.

Fagiano, L., Quack, M., Bauer, F., Carnel, L., and Oland, E. (2021). Autonomous airborne wind energy systems: Accomplishments and challenges. *Annu. Rev. Control. Robotics Auton. Syst.*, 5, 603–631.

Loyd, M.L. (1980). Crosswind kite power. *J. Energy*, 4, 106–11.

Ranneberg, M. (2013). Sensor setups for state and wind estimation for airborne wind energy converters. *CoRR*, abs/1309.1029.

Schmidt, E., De Lellis Costa De Oliveira, M., Saraiva Da Silva, R., Fagiano, L., and Trofino Neto, A. (2020). In-Flight Estimation of the Aerodynamics of Tethered Wings for Airborne Wind Energy. *IEEE Transactions on Control Systems Technology*, 28(4), 1309–1322. doi: 10.1109/TCST.2019.2907663.